Implication of grain-boundary structure and chemistry on plasticity and failure

Gerhard Dehm* and Julie Cairney

Failure processes are often linked to interfaces, their atomistic structure and chemistry. Therefore, a detailed understanding of failure processes requires knowledge of structural and chemical interface states as a prerequisite. Recent advances in transmission electron microscopy and atom probe tomography allow this information to be gathered with the highest spatial and chemical resolution. Insights on how strength, ductility, and toughness can be manipulated by grain-boundary complexions (i.e., grain-boundary state transitions) due to their impact on grain-boundary cohesion as well as dislocation–grain-boundary interaction processes have been recently gained. Making use of the multidimensional space spanned by grain boundaries concerning their atomic structure, chemical composition, grain-boundary inclinations and defects will enable new concepts for grain-boundary engineering of mechanical properties.

Introduction

Grain boundaries impact nearly all material properties, which is usually represented by simply referring to the mean grain size d as the controlling property parameter. As an example, the coercivity of magnetic materials scales with 1/d down to approximately the width of a Bloch domain wall. Below this critical dimension, the grain size–coercivity scaling changes to d^6 due to an altered domain wall pinning mechanism.[1] Similarly, strength increases with decreasing grain size, as utilized in fine-grained and nanocrystalline materials, where grain boundaries obstruct the path of dislocations.[2] Again, below a certain dimension in the range of 10 nm, the deformation mechanism alters from dislocation–grain-boundary interactions to grain-boundary sliding and shear coupled grain-boundary motion,[3] causing a softening.

Often grain boundaries are treated as one type of defect among others in materials. This is usually based on generalized (continuums) trends deduced from macroscopic property measurements. However, grain boundaries have a rich "cosmos" in atomic structure, chemistry, and secondary grain-boundary defects (steps, facets, grain-boundary dislocations,…) spanning a multidimensional space[4] considering all the above-mentioned aspects and for this reason, individual grain boundaries in a polycrystalline material are expected to behave differently. Recent examples show this for the electrical resistivity of grain boundaries in pure Cu[5] or thermal stability against grain growth in Cu-Zr alloys.[6,7]

The chemistry of grain boundaries directly affects equilibrium properties such as grain-boundary energy, entropy, and enthalpy, as well as their nonequilibrium properties, such as mobility, cohesive strength, and grain-boundary diffusion and sliding resistance. The composition therefore affects not only the properties, but also materials processing and microstructure development. Just using 'd' is often not enough, and to shed light on the property variations imposed by grain boundaries a detailed knowledge of their structure and chemistry is a prerequisite.

This article focuses first on the methods to probe the structure and chemistry of GBs by atomic resolved transmission electron microscopy (TEM) techniques and atom probe tomography (APT), which offer unprecedented spatial and chemical resolution. We will then address localized experiments and atomistic simulations for a detailed understanding on the impact of individual grain boundaries on strength and failure. The overview includes the paradigm change that grain boundaries exist in multiple states (complexions) and how this opens new ways to alter mechanical properties.

Gerhard Dehm, Max-Planck-Institut für Eisenforschung GmbH, Düsseldorf, Germany; dehm@mpie.de
Julie Cairney, Australian Centre for Microscopy and Microanalysis, The University of Sydney, Sydney, Australia; julie.cairney@sydney.edu.au
*Corresponding author

doi:10.1557/s43577-022-00378-3

Grain boundaries: From geometry to grain-boundary structure and complexions

Grain boundaries are classified by their five macroscopic degrees of freedom. Three are required to describe the orientation relationship between the two abutting grains and two for the orientation of the grain-boundary plane (**Figure 1**). The latter is required as, for the same misorientation, different grain-boundary inclinations (planes) can occur (Figure 1a–b). Rigid body translations in x, y, and z directions finally describe the atomic coordinates of a grain boundary (microscopic degrees of freedom).[6] Tilt, twist, or mixed boundaries occur and, depending on the misorientation angle, low-angle and high-angle grain boundaries (LAGBs, HAGBs) are discriminated. LAGBs are described by Read and Shockley as a dislocation network that can accommodate the misorientation between the two grains.[8] With increasing misorientation, the dislocation spacing gets smaller, until they can no longer be accommodated (typically ~15°). At specific misorientations coincidence sites occur for the abutting grains. This superstructure can be found by overlapping both lattice structures creating a coincidence site lattice (CSL) (Figure 1c). Grain boundaries originating from a CSL are described by their frequency of coincidence sites with respect to total lattice sites expressed as a ∑value. For example, a common twin boundary in fcc metals shares every third lattice position and is termed a ∑3 HAGB. The ∑3 twin boundary can exist at different macroscopic inclinations; the {111} and {112} are the most common, forming a symmetric HAGB. Symmetric CSL grain boundaries (i.e., both grains share the same grain-boundary plane, can be described by repeating structural units [Figure 1d]).

Grain boundaries can be also described by Gibbsian thermodynamics using the interfacial excess properties: excess energy [U], excess entropy [S], excess volume [V], the grain-boundary excess [N_i] of component i at the grain boundary and the grain-boundary free energy γ. The free grain-boundary energy was recently elegantly formulated by Frolov and Mishin as a function of pressure (stress), temperature, and chemical potentials of the components (composition).[9] The conditions for grain-boundary phase transitions require that in equilibrium both states coexist (these grain-boundary phases are also called "complexions"[10,11] to avoid confusion with bulk phase transitions). A change in temeprature, pressure (stress), and/or chemical composition (including point defects) will then induce a transition from a specific grain-boundary phase to another (see Figure 1e–f), that is, a specific atomic structure with a certain excess of the components in the system (e.g., segregation of impurities) will be stabilized. As a consequence, these parameters can be used to manipulate grain-boundary structures and/or compositions, and thus impact material properties.

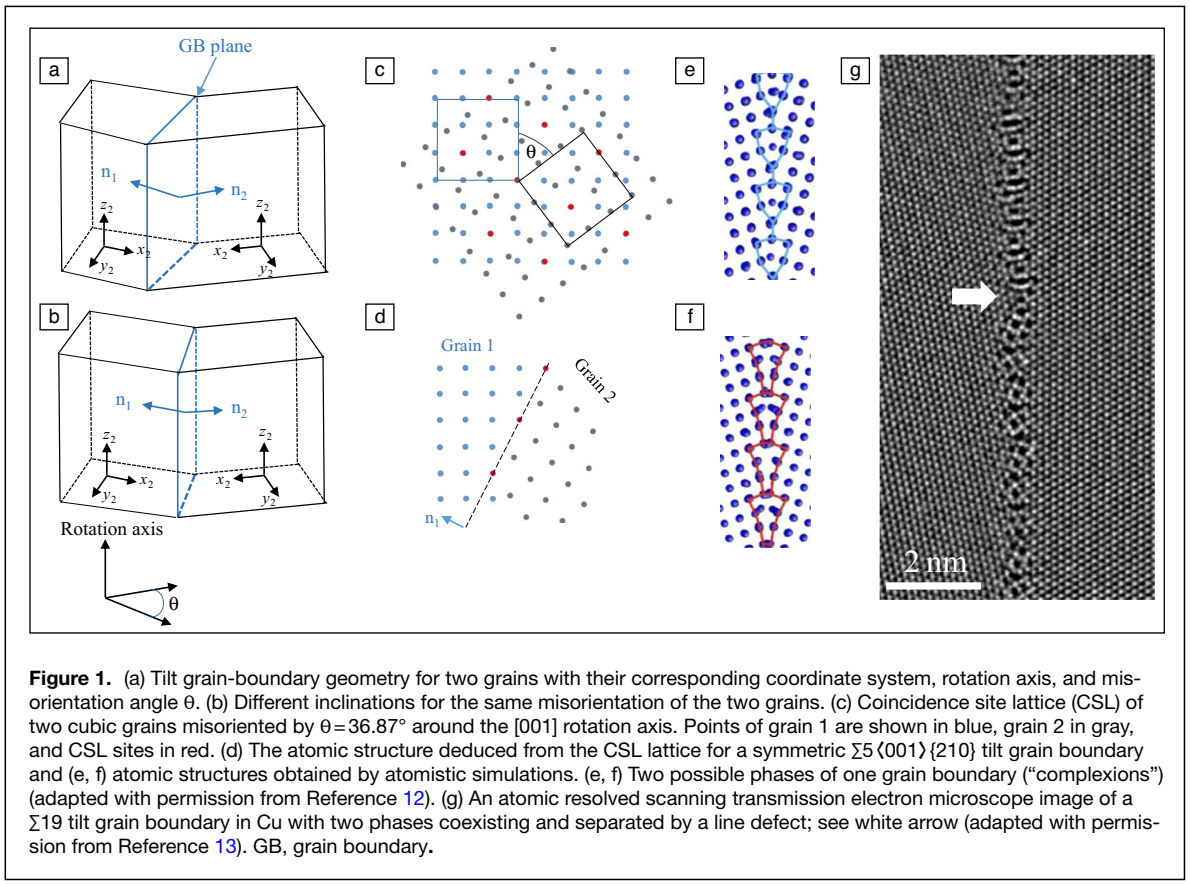

Figure 1. (a) Tilt grain-boundary geometry for two grains with their corresponding coordinate system, rotation axis, and misorientation angle θ. (b) Different inclinations for the same misorientation of the two grains. (c) Coincidence site lattice (CSL) of two cubic grains misoriented by θ = 36.87° around the [001] rotation axis. Points of grain 1 are shown in blue, grain 2 in gray, and CSL sites in red. (d) The atomic structure deduced from the CSL lattice for a symmetric ∑5⟨001⟩{210} tilt grain boundary and (e, f) atomic structures obtained by atomistic simulations. (e, f) Two possible phases of one grain boundary ("complexions") (adapted with permission from Reference 12). (g) An atomic resolved scanning transmission electron microscope image of a ∑19 tilt grain boundary in Cu with two phases coexisting and separated by a line defect; see white arrow (adapted with permission from Reference 13). GB, grain boundary.

Resolving grain-boundary structure and composition by TEM and APT: Basics and recent insights

The recent advances of aberration correction TEM and scanning TEM (STEM) techniques enable us to resolve atomic structures down to ~50 pm with precision of a few pm in atomic positions.[14] Structural units of CSL boundaries are easily resolved if both grains are aligned along a common zone axis and the boundary is flat through the thickness of the sample. High-angle annular dark-field (HAADF)–STEM is often employed, as the elastically and incoherently scattered electrons provide intensity distributions I as a function of atomic number Z with $I \sim Z$.[2,14] Z-contrast imaging allows the determination of the atomic structure of grain boundaries and whether their substitutional sites are preferentially occupied by segregates.

Recently, Meiners et al.[13] revealed by HAADF–STEM that pure Cu grain boundaries can possess different atomic structures, demonstrated by findings for asymmetric and symmetric ∑19[111] grain boundaries (Figure 1g). Atomistic simulations confirmed that both states possess different excess state variables such as excess volume.[13] Although for many grain-boundary transitions, temperature is the decisive parameter,[15] stress triggers the transitions between both states here.[13] Earlier, Monte Carlo coupled molecular dynamics (MC/MD) simulations predicted, for Cu ∑5[001], two separate grain-boundary phases possessing different kite structure motifs (Figure 1e–f) at different temperatures.[12] Although the three-dimensional atomic structure can be readily resolved by atomistic simulations, this is still in its infancy for STEM, with current progress reported in References 16–18. Recently, Du et al. were the first to report on grain-boundary structures resolved in three dimensions at the atomic level by STEM tomography, providing quantitative access to coordination and bonding angle of atoms located at the grain boundary and within the grains in Au.[19]

Chemically induced transitions can be complex and include sub-monolayer to multilayer segregation, as found for alumina ceramics[11] resolved by STEM. Other examples for metallic materials include ordered segregation for Cu-Bi,[20–23] Ni-Bi,[24] nanofaceting for Cu-Ag[25,26] and Cu-Bi,[27] and order–disorder transitions for Cu-Zr,[7,28] Ni-S,[23] and multielement systems.[29–31]

Atom probe tomography (APT) is a powerful microscopy technique that provides three-dimensional maps that show the distribution of atoms of different elements at the nanometer length scale.[32] Needle-shaped samples are exposed to a pulsed local field and atoms are individually field-evaporated. A position-sensitive single atom detector provides data that are reconstructed to create maps of needle-shaped volumes with a diameter of ~100 nm that can be several microns long. Depending on the sample, the resolution of the technique is around 0.1–0.3 nm along the direction of the needle and 0.3–0.5 nm laterally.

Although the resolution at grain boundaries is not generally sufficient to resolve the grain-boundary structure, APT has proven to be a very useful technique for resolving grain-boundary composition and identifying and measuring complexions. The inherently three-dimensional nature of the data overcomes a limitation of beam-based techniques that require the interface to be flat along one orientation, running exactly parallel to the direction of the beam. Grain-boundary excess values can be calculated from atom probe data by partitioning the data and measuring the local composition at the boundaries and in the adjacent grains.

Using atom probe to map the composition across grain boundaries[33] has revealed that the composition of grain boundaries varies highly across individual boundaries, and between adjacent boundaries, where local composition is influenced by the local boundary structure (**Figure** 2). Atom probe can also be used to discern and measure the segregation to the individual dislocations that comprise low-angle boundaries (Figure 2a) and to compare segregation at special boundaries, such as twins, which tend to have lower segregation levels than high-angle boundaries. APT, combined with TEM, has been used to identify complexions such as segregation-induced faceting transitions[34–36] and spinodal-like fluctuations.[37]

Atom probe has also been used to demonstrate the existence of linear complexions along dislocations[34] and to study other planar structural defects such as stacking faults[38] and antiphase boundaries.[39]

Grain boundaries and their impact on plasticity

Although the strength of metallic materials increases with decreasing grain size according to the Hall–Petch equation, it is well known that plasticity is not only affected by dislocations piling up at grain boundaries, but equally important are absorption, emission, nucleation, and transmission processes. Dislocation transmission through grain boundaries can be understood on a continuums level by considering the orientation difference between incoming and outgoing glide systems, as this determines the magnitude of the residual Burgers vector, which must be accommodated (**Figure** 3a). Additionally, the resolved shear stress acting on these glide systems must be considered.[42–45] *In situ* and postmortem TEM studies have shed fundamental light on dislocation–grain-boundary interaction mechanisms (e.g.,[46] see Figure 3f–h), but the limited volume and small TEM sample thickness often alter stresses compared to the bulk.

Another approach to study the impact of grain boundaries on plasticity uses nanoindentation[47] or micromechanical testing of bicrystalline pillars.[48–55] The advantage of the latter method is that slip steps on the pillar side surface(s) can be analyzed and the activated and transmitted glide systems resolved (Figure 3b–c).

The mechanical signal deduced from the load–displacement curves is not always straightforward to interpret due to the stochastic nature of small-scale plasticity. Often large data sets and different pillar dimensions are required to draw

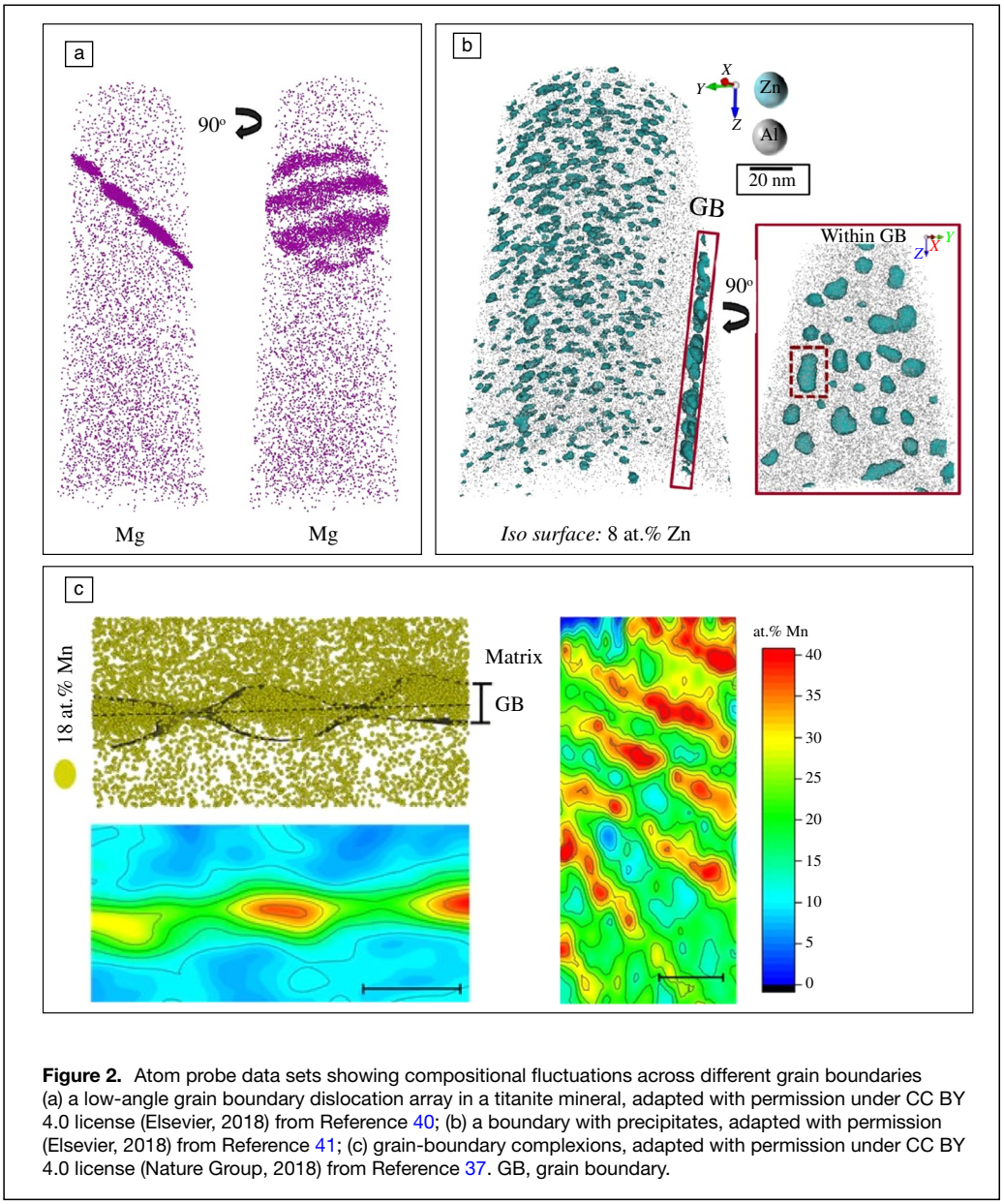

Figure 2. Atom probe data sets showing compositional fluctuations across different grain boundaries (a) a low-angle grain boundary dislocation array in a titanite mineral, adapted with permission under CC BY 4.0 license (Elsevier, 2018) from Reference 40; (b) a boundary with precipitates, adapted with permission (Elsevier, 2018) from Reference 41; (c) grain-boundary complexions, adapted with permission under CC BY 4.0 license (Nature Group, 2018) from Reference 37. GB, grain boundary.

conclusions. For example, the transmission stress for easy slip transmission across a $\sum 3$ (111) twin boundary in Cu seems to be similar to the stress required for cross-slip according to experimental findings,[52] thus leaving none or only a small fingerprint in stress–strain data in contrast to impenetrable grain boundaries (Figure 3d–e). A point largely overlooked so far in the experimental community is the strain rate sensitivity of dislocation transmission. This becomes a crucial factor when thermally assisted processes are involved in the transmission process as shown in Reference 56. The impact of different grain-boundary phases of pure or alloyed systems in experimental small-scale mechanical testing is still in its infancy.

On the other end, macroscopic mechanical tests provide an average of the strength over multiple grain boundaries. Nevertheless, again helpful insights were obtained. Prominent examples are nanocrystalline Cu-Zr samples, where the phase state of multiple grain boundaries was changed by different quenching rates after a 950°C annealing treatment. In this process, Zr enriched at the grain boundaries formed either preferentially ordered grain-boundary structures (slow cooling) or amorphous grain-boundary structures (fast cooling).[7] These two different grain-boundary phase states—ordered versus amorphous—impacted the strength and ductility. The nanocrystalline sample with predominantly amorphous grain-boundary structures outperformed the Cu-Zr sample with mainly ordered grain-boundary structures with respect to compressive strength and strain to failure upon bending,[7] whereas the average grain size remained unaltered.

Atomistic simulations reveal differences in dislocation nucleation, dislocation pinning, and crack arresting ability for both types of grain-boundary phases.[57,58] This opens up an interesting design route in nanocrystalline materials, for which strength usually increases as dislocation multiplication diminishes, causing at the same time a severe reduction in strain to failure under tensile loading. Assisting dislocation nucleation by a change in excess volume, pinning dislocations at grain-boundary ledges, altering the density of grain-boundary ledges for certain segregation content (excess) and distribution (atomistic), as well as altering cohesive grain-boundary strength are scenarios discussed in the community.

Grain-boundary-dominated failure: Origin and solutions

Fracture toughness in metals is governed by two main mechanisms: micro-ductile crack propagation and crack propagation by de-cohesion. Both are affected by the atomic-scale structure and composition of grain boundaries. In the case of micro-ductile crack propagation, the impact

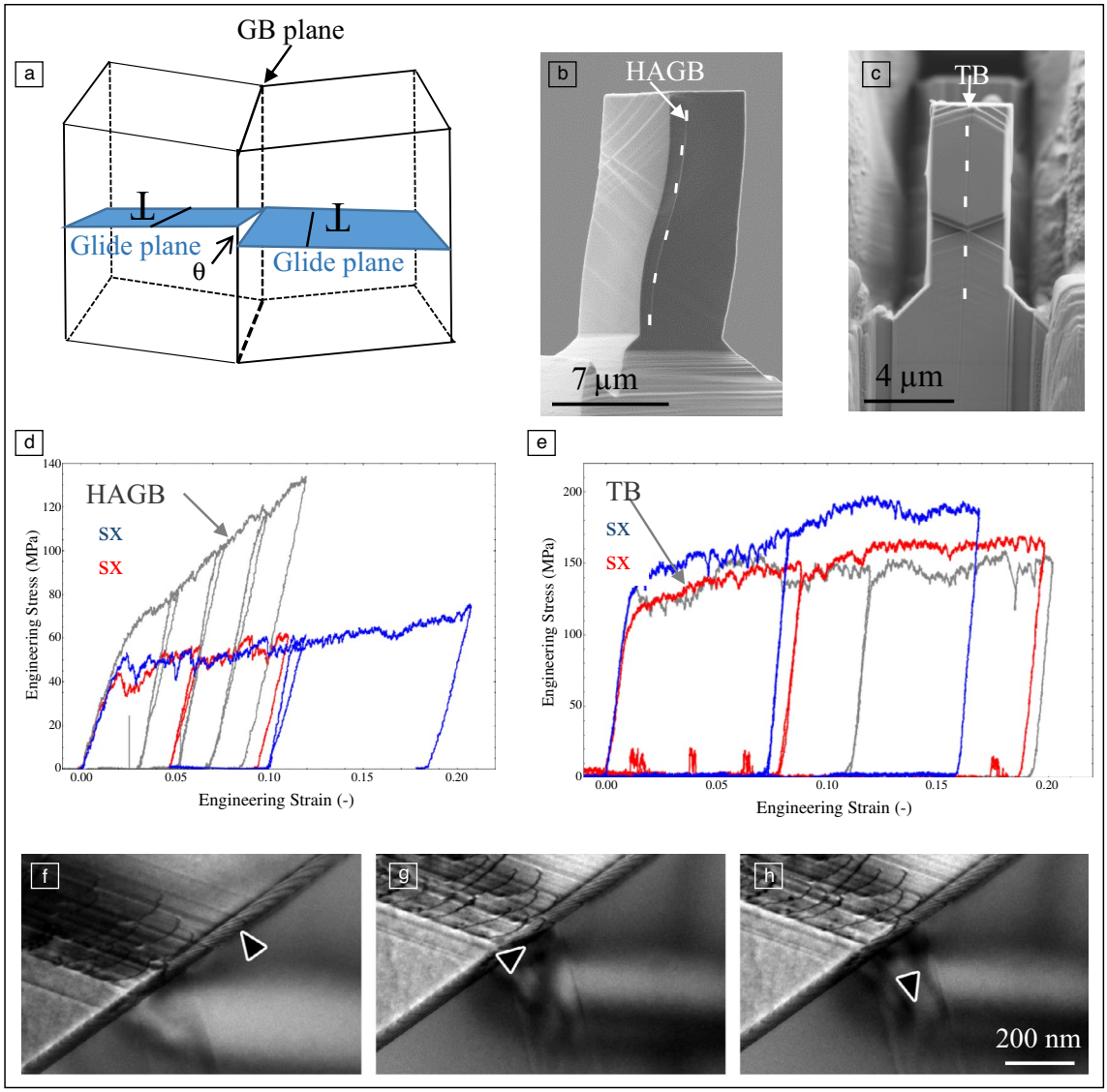

Figure 3. (a) Schematic illustrating the misalignment of slip planes across a grain boundary (GB). As a consequence, dislocation lines need to realign and a residual Burgers vector will be stored in the GB. Also the critical resolved shear stresses can be different for incoming and outgoing dislocations. Scanning electron microscope image of a (b) high-angle grain boundary (HAGB) with a low transmission factor causing severe distortion of the pillar even after only ~8% engineering strain in contrast to a (c) coherent twin boundary (TB) deformed to ~19% strain, where slip steps meet at the TB indicating slip transmission. (d, e) Corresponding stress–strain curves of the HAGB and TB copper pillars in comparison to single-crystal (sx) copper samples of according dimensions. Note the strong apparent hardening of the HAGB, which is absent for the pillar containing the TB. (f–h) Transmission electron microscope images of dislocation–TB interaction in 304 stainless steel.[46] Arrowheads indicate position of (f) cross-slip into the TB plane and (g, h) transmission across the TB. Images (b–e) reprinted with permission in modified form from Imrich et al.[59] and (f–h) from Reference 46.

of grain boundaries varies. They act as obstacles for dislocation glide, but the intersection points with the crack front can also act as preferred sites for dislocation nucleation. Reiser and Hartmaier[60] recently modeled these competing effects by means of two-dimensional discrete dislocation dynamics, concluding that the positive impact of grain boundaries outweighs the negative consequences of dislocation blocking. In samples that have a preferred crack path within a grain (such as a crystallographic cleavage plane or an interphase interface), the changes in orientation of the crack path at grain boundaries can enhance toughness.[61]

For materials in which failure occurs as the result of cracks that propagate along grain boundaries, the macroscopic fracture strength depends strongly on the microscopic structure of the boundaries, including both the geometry and composition. The energetic barrier to intergranular failure is the grain-boundary cohesive energy:

$$E_{GBC} = 2\gamma_S - \gamma_{GB}, \quad (1)$$

where E_{GBC} is the grain-boundary cohesion energy, γ_S is the surface energy, and γ_{GB} is the grain-boundary energy.[62]

The structure of a grain boundary influences this energy. Experiments and calculations have confirmed the patterns of structural units are key to understanding the boundary energy.[63] Although the relationship is complex, a clear trend is that the energy of structural units is related to the excess free volume of the units. In particular, special boundaries have a higher barrier to intergranular failure due to their lower boundary energy, which is derived from the lower excess free volume.

Watanabe proposed the concept of "grain-boundary engineering" for the design of materials with the desired properties.[64] This approach focuses on the type of grain boundaries (low angle, high angle, special, etc.), designing materials with an optimum combination of grain-boundary types in order to achieve the desired properties. In real materials, the fracture strength is further complicated by impurities at the interface, emission of dislocations during fracture, and more complex geometries such as triple junctions, which can also be fracture nucleation sites.

Specifically, composition plays an extremely important role, so much so that the concept of "grain-boundary segregation engineering" was proposed by Raabe in 2014.[65] This involves manipulating grain boundaries via solute decoration enabling changes in energy, mobility, structure, and cohesion or even promoting local phase transformation to enable useful material behavior. In nanocrystalline materials, for which the volume fraction of grain boundaries is extremely high, the importance of considering grain-boundary composition is even more pronounced.[66]

Of course, segregation is influenced by structure, so the two effects are inextricably linked. The free volume at grain boundaries means that boundaries contain lower-energy sites for solute atoms than the bulk. APT is an extremely sensitive tool for measuring grain-boundary segregation, and over many years of studying engineering alloys with this technique, we have learned that it is extremely rare to find boundaries in engineering alloys without some level of segregation of solute or impurities. Industrial alloy systems usually contain both equilibrium segregation (i.e., solutes at grain boundaries themselves as a result of the decrease of the interfacial free energy of the boundary when impurity atoms are present) and nonequilibrium segregation in the vicinity of the boundary (i.e., changes in composition in the vicinity of the boundary that result from the diffusion of vacancies and atoms toward/away from the boundary). APT is an excellent tool to study the equilibrium segregation at the interface itself. Nonequilibrium segregation occurs over length scales on the micrometer scale, which is larger than a typical atom probe data set (100 nm across), and is better observed by using NanoSIMS, a highly sensitive tool that provides two-dimensional maps over a larger area. As an example, in a study of segregation of B, P, and C in the Ni-Based Superalloy, Inconel 718 (which has dramatic effects of the welding properties), NanoSIMS was able to reveal nonequilibrium segregation of B, but local, equilibrium, segregation of P and C was only able to be observed by atom probe.[67]

There are countless examples of systems in which the local grain-boundary composition affects fracture properties. Many are cases in which certain species embrittle alloys systems (e.g., P, N, and S in steel, Bi in Cu, S in Ni), but in some cases the effect can be a beneficial increase in ductility (Fe, B and C in Mo,[68] and Re in W.[69] A well-known scenario is the case of liquid metal embrittlement, whereby normally ductile metals become extremely brittle in the presence of liquid metals. Classic examples include steels becoming brittle in the presence of liquid Zn,[70] which can happen if Zn-coated samples are welded, and Al becoming brittle in the presence of liquid Ga.[71]

Creating alloys with superior properties through grain-boundary segregation engineering requires an understanding of the atomistic processes that govern this behavior. In 2018, Leitner et al.[68] investigated the fracture behavior of Mo-Hf alloys, which display a transition from intergranular to transgranular fracture above 2% Hf. Atom probe observations of grain boundaries revealed that the grain-boundary strength was, in fact, affected by O, C, and B impurities at the boundary, rather than Hf itself (**Figure** 4). Increased Hf actually leads to a greater C and B enrichment, and less O at boundaries, increasing the cohesion. Density functional theory (DFT) modeling revealed the underlying segregation energetics, explaining the changes in solute excess observed at the boundaries. Atomic-scale insights provided unexpected new

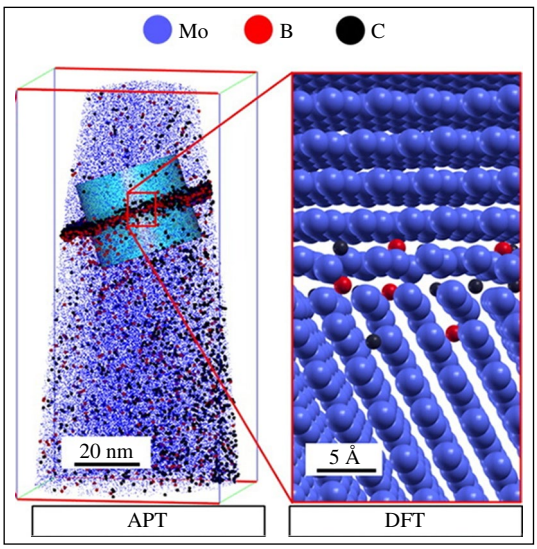

Figure 4. Atom probe data set and a density functional theory (DFT) representation of a Mo-Hf alloy in which grain-boundary chemistry controls the failure mode. Figure adapted with permission (Elsevier, 2018) from Reference 68. APT, atom probe tomography.

perceptions that can guide alloy design, taking advantage of impurity-level additions of C and B, or developing strategies to reduce O, to improve the properties of this system.

Conclusion

Grain boundaries are central to plastic deformation and failure in metals and alloys. Traditionally, only average grain size d is considered, perhaps together with the grain shape or texture, but grain-boundary geometry, structure, and composition play at least an equally important role, in some cases, trumping grain size. Recent advances in the capabilities of microscopy techniques, including advanced TEM and APT, are able to provide essential atomic-scale structural and chemical information for the effective design of materials with desired properties. These new insights open the path for true grain-boundary engineering, considering the multidimensional nature of a boundary's structure, composition, complexions, inclinations, and defects.

Acknowledgments

G.D. acknowledges financial support by the ERC Advanced Grant GB-Correlate (Grant No. 787446-GB-CORRELATE) and the Deutsche Forschungsgemeinschaft (DFG) through the project B06 of the SFB1394 Structural and Chemical Atomic Complexity—From Defect Phase Diagrams to Material Properties (Project ID 409476157). Stimulating discussions on the topic of grain boundaries with many colleagues, especially C. Kirchlechner, T. Brink, and C. Liebscher are gratefully acknowledged by G.D. J.M.C. acknowledges the support of an ARC Future Fellowship (FT180100232).

Funding

Open Access funding enabled and organized by Projekt DEAL.

Data availability

All data presented in this overview article have been published previously and can be obtained from the corresponding references.

Conflict of interest

The authors state that there are no conflicts of interest.

Open Access

References

1. G. Herzer, *Phys. Scr.* **T49A**, 307 (1993)
2. E. Arzt, *Acta Mater.* **46**, 5611 (1998)
3. J. Han, S.L. Thomas, D.J. Srolovitz, *Prog. Mater Sci.* **98**, 386 (2018)
4. W.D. Kaplan, D. Chatain, P. Wynblatt, W.C. Carter, *J. Mater. Sci.* **48**, 5681 (2013)
5. H. Bishara, S. Lee, T. Brink, M. Ghidelli, G. Dehm, *ACS Nano* **15**, 16607 (2021)
6. P.R. Cantwell, T. Frolov, T.J. Rupert, A.R. Krause, C.J. Marvel, G.S. Rohrer, J.M. Rickman, M.P. Harmer, *Annu. Rev. Mater. Res.* **50**, 465 (2020)
7. A. Khalajhedayati, Z. Pan, T.J. Rupert, *Nat. Commun.* **7**, 10802 (2016)
8. W.T. Read, W. Shockley, *Phys. Rev.* **78**, 275 (1950)
9. T. Frolov, Y. Mishin, *Phys. Rev. B* **8**(5), 224107 (2012)
10. M. Tang, W.C. Carter, R.M. Cannon, *Phys. Rev. Lett.* **97**, 075502 (2006)
11. S.J. Dillon, M. Tang, W.C. Carter, M.P. Harmer, *Acta Mater.* **55**, 6208 (2007)
12. T. Frolov, S.V. Divinski, M. Asta, Y. Mishin, *Phys. Rev. Lett.* **110**, 255502 (2013)
13. T. Meiners, T. Frolov, R.E. Rudd, G. Dehm, C.H. Liebscher, *Nature* **579**, 375 (2020)
14. S.J. Pennycook, P.D. Nellist, *Scanning Transmission Electron Microscopy: Imaging and Analysis* (Springer, Berlin, 2011)
15. G.S. Rohrer, *Curr. Opin. Solid State Mater. Sci.* **20**, 231 (2016)
16. Z. Saghi, P.A. Midgley, *Annu. Rev. Mater. Res.* **42**, 59 (2012)
17. S. Van Aert, K.J. Batenburg, M.D. Rossell, R. Erni, G. Van Tendeloo, *Nature* **470**, 374 (2011)
18. E. Arslan Irmak, P. Liu, S. Bals, S. Van Aert, *Small Methods* **5**, 2101150 (2021)
19. C. Wang, H. Duan, C. Chen, P. Wu, D. Qi, H. Ye, H.-J. Jin, H.L. Xin, K. Du, *Matter* **3**, 1999 (2020)
20. G. Duscher, M.F. Chisholm, U. Alber, M. Rühle, *Nat. Mater.* **3**, 621 (2004)
21. R. Schweinfest, A.T. Paxton, M.W. Finnis, *Nature* **432**, 1008 (2004)
22. A. Kundu, K.M. Asl, J. Luo, M.P. Harmer, *Scr. Mater.* **68**, 146 (2013)
23. T. Hu, S. Yang, N. Zhou, Y. Zhang, J. Luo, *Nat. Commun.* **9**, 2764 (2018). https://doi.org/10.1038/s41467-018-05070-2
24. J. Luo, H. Cheng, K.M. Asl, C.J. Kiely, M.P. Harmer, *Science* **333**, 1730 (2011)
25. N.J. Peter, M.J. Duarte, C. Kirchlechner, C.H. Liebscher, G. Dehm, *Acta Mater.* **214**, 116960 (2021)
26. N.J. Peter, T. Frolov, M.J. Duarte, R. Hadian, C. Ophus, C. Kirchlechner, C.H. Liebscher, G. Dehm, *Phys. Rev. Lett.* **121**, 255502 (2018). https://doi.org/10.1103/PhysRevLett.121.255502
27. W. Sigle, L.-S. Ciiang, W. Gusr, *Philos. Mag. A* **82**(8), 1595 (2002)
28. T. Meiners, J.M. Duarte, G. Richter, G. Dehm, C.H. Liebscher, *Acta Mater.* **190**, 93 (2020)
29. F. Cao, Y. Chen, S. Zhao, E. Ma, L. Dai, *Acta Mater.* **209**, 116786 (2021)
30. S. Rajeshwari, S. Sankaran, K.C. Hari Kumar, H. Rösner, M. Peterlechner, V.A. Esin, S. Divinski, G. Wilde, *Acta Mater.* **195**, 501 (2020)
31. A. Ahmadian, D. Scheiber, X. Zhou, B. Gault, C.H. Liebscher, L. Romaner, G. Dehm, *Nat. Commun.* **12**, 6008 (2021)
32. B. Gault, M.P. Moody, J.M. Cairney, S.P. Ringer, *Atom Probe Microscopy* (Springer, Berlin, 2012)
33. P. Felfer, B. Scherrer, J. Demeulemeester, W. Vandervorst, J.M. Cairney, *Ultramicroscopy* **159**, 438 (2015)
34. C.H. Liebscher, A. Stoffers, M. Alam, L. Lymperakis, O. Cojocaru-Mirédin, B. Gault, J. Neugebauer, G. Dehm, C. Scheu, D. Raabe, *Phys. Rev. Lett.* **121**, 015702 (2018)
35. N.J. Peter, T. Frolov, M.J. Duarte, R. Hadian, C. Ophus, C. Kirchlechner, C.H. Liebscher, G. Dehm, *Phys. Rev. Lett.* **121**, 255502 (2018)
36. H. Zhao, L. Huber, W. Lu, N.J. Peter, D. An, F. De Geuser, G. Dehm, D. Ponge, J. Neugebauer, B. Gault, *Phys. Rev. Lett.* **124**, 106102 (2020)
37. A. Kwiatkowski da Silva, D. Ponge, Z. Peng, G. Inden, Y. Lu, A. Breen, B. Gault, D. Raabe, *Nat. Commun.* **9**, 1 (2018)
38. R. Herschitz, D. Seidman, *Acta Metall.* **33**, 1547 (1985)
39. S.K. Makineni, M. Lenz, S. Neumeier, E. Spiecker, D. Raabe, B. Gault, *Scr. Mater.* **157**, 62 (2018)
40. C.L. Kirkland, D. Fougerouse, S.M. Reddy, J. Hollis, D.W. Saxey, *Chem. Geol.* **483**, 558 (2018)
41. H. Zhao, F. De Geuser, A. Kwiatkowski da Silva, A. Szczepaniak, B. Gault, D. Ponge, D. Raabe, *Acta Mater.* **156**, 318 (2018)
42. J.D. Livingston, B. Chalmers, *Acta Metall.* **5**, 322 (1957)
43. E. Werner, W. Prantl, *Acta Metall. Mater.* **38**, 533 (1990)

44. W.A.T. Clark, R.H. Wagoner, Z.Y. Shen, T.C. Lee, I.M. Robertson, H.K. Birnbaum, *Scr. Metall. Mater.* **26**, 203 (1992)
45. I.J. Beyerlein, M.J. Demkowicz, A. Misra, B.P. Uberuaga, *Prog. Mater Sci.* **74**, 125 (2015)
46. J. Kacher, B.P. Eftink, B. Cui, I.M. Robertson, *Curr. Opin. Solid State Mater. Sci.* **18**, 227 (2014)
47. F. Javaid, H. Pouriayevali, K. Durst, *J. Mater. Res.* **36**, 2545 (2021)
48. G. Dehm, B.N. Jaya, R. Raghavan, C. Kirchlechner, *Acta Mater.* **142**, 248 (2018)
49. N. Kheradmand, A. Barnoush, H. Vehoff, *J. Phys. Conf. Ser.* **240**, 012017 (2010)
50. N. Kheradmand, H. Vehoff, A. Barnoush, *Acta Mater.* **61**, 7454 (2013)
51. P.J. Imrich, C. Kirchlechner, C. Motz, G. Dehm, *Acta Mater.* **73**, 240 (2014)
52. N.V. Malyar, B. Grabowski, G. Dehm, C. Kirchlechner, *Acta Mater.* **161**, 412 (2018)
53. J.S. Weaver, N. Li, N.A. Mara, D.R. Jones, H. Cho, C.A. Bronkhorst, S.J. Fensin, G.T. Gray, *Acta Mater.* **156**, 356 (2018)
54. A. Kunz, S. Pathak, J.R. Greer, *Acta Mater.* **59**, 4416 (2011)
55. K.S. Ng, A.H.W. Ngan, *Philos. Mag.* **89**, 3013 (2009)
56. N.V. Malyar, G. Dehm, C. Kirchlechner, *Scr. Mater.* **138**, 88 (2017)
57. V. Turlo, T.J. Rupert, *Acta Mater.* **151**, 100 (2018)
58. P. Garg, Z. Pan, V. Turlo, T.J. Rupert, *Acta Mater.* **218**, 117213 (2021)
59. P.J. Imrich, C. Kirchlechner, D. Kiener, G. Dehm, *Scr. Mater.* **100**, 94 (2015)
60. J. Reiser, A. Hartmaier, *Sci. Rep.* **10**, 2739 (2020)
61. S. Kumar, W.A. Curtin, *Mater. Today* **10**, 34 (2007)
62. D. McLean, *Grain Boundaries in Metals* (Clarendon Press, Oxford, 1957)
63. V.R. Coffman, J.P. Sethna, *Phys. Rev. B* **77**, 144111 (2008)
64. T. Watanabe, *J. Mater. Sci.* **46**, 4095 (2011)
65. D. Raabe, M. Herbig, S. Sandlöbes, Y. Li, D. Tytko, M. Kuzmina, D. Ponge, P.P. Choi, *Curr. Opin. Solid State Mater. Sci.* **18**, 253 (2014)
66. T. Chookajorn, H.A. Murdoch, C.A. Schuh, *Science* **337**, 951 (2012)
67. T. Alam, P.J. Felfer, M. Chaturvedi, L.T. Stephenson, M.R. Kilburn, J.M. Cairney, *Metall. Mater. Trans. A.* **43A**, 2183 (2012)
68. K. Leitner, D. Scheiber, S. Jakob, S. Primig, H. Clemens, E. Povoden-Karadeniz, L. Romaner, *Mater. Des.* **142**, 36 (2018)
69. B. Gludovatz, S. Wurster, A. Hoffmann, R. Pippan, *Int. J. Refract. Metals Hard Mater.* **28**, 674 (2010)
70. M. Razmpoosh, C. DiGiovanni, Y. Zhou, E. Biro, *Prog. Mater Sci.* **121**, 100798 (2021)
71. W. Sigle, G. Richter, M. Rühle, S. Schmidt, *Appl. Phys. Lett.* **89**, 121911 (2006) □

Gerhard Dehm is a director at the Max-Planck-Institut für Eisenforschung in Düsseldorf and a professor at the Ruhr Universität Bochum, Germany. His research focuses on mechanical properties of materials and their microstructure origin, which his research team investigates with miniaturized mechanical experiments and advanced electron microscopy methods. He was recently awarded a European Research Council Advanced Grant to correlate the state and properties of grain boundaries. Dehm can be reached by email at dehm@mpie.de.

Julie Cairney is a professor of materials engineering at The University of Sydney, Australia. She is also the University's Pro Vice Chancellor for Research Enterprise and Engagement. She leads a research group that specializes in using advanced microscopy to study the three-dimensional structure of materials at the atomic scale. Her projects cover steels, light alloys, corrosion, geological materials, and biominerals. In 2020, she was awarded the Acta Materialia Silver Medal for her contributions to materials science research. Cairney can be reached by email at julie.cairney@sydney.edu.au.